2017 International Conference on
Unmanned Aircraft Systems (ICUAS)
June 13-16, 2017, Miami, FL, USA

Improving Quadrotor Trajectory Tracking by Compensating for Aerodynamic Effects

James Svacha Kartik Mohta Vijay Kumar

***Abstract*— In this work, we demonstrate that the position tracking performance of a quadrotor may be significantly improved for forward and vertical flight by incorporating simple lumped parameter models for induced drag and thrust, respectively, into the quadrotor dynamics and modifying the controller to compensate for these terms. We further show that the parameters for these models may be easily and accurately identified offline from forward and vertical flight data. We demonstrate that the simple drag compensating controller can reduce the position error in the direction of forward flight in steady state by 75%, and that the controller using a more accurate thrust model, dubbed the "refined" thrust model, can improve the position error by 72% in the vertical direction.**

I. Introduction

The use of micro-aerial vehicles and especially quadrotors has seen a rapid growth in the past few years. These vehicles have been used in various applications such as aerial photography, surveillance, inspection of structures [1], and even agricultural monitoring [2]. Future applications involve search and rescue and emergency response [3]. One of the main advantages of aerial vehicles over ground based ones is the ability to move quickly in 3D environments unhindered by rugged terrain.

During high speed and even moderate flight regimes, quadrotors are affected by a variety of aerodynamic effects such as blade flapping, induced drag, and thrust variation due to changes in induced velocity. As the speed of the quadrotor increases, these aerodynamic effects become more significant and start affecting the control of the robot. Because we wish to use quadrotors to complete time sensitive tasks, we need to fly in regimes in which these aerodynamics effects are not negligible. To maintain precise control of the quadrotor, we need to accurately model and compensate for these aerodynamic effects.

The aerodynamics of quadrotors have not received as much interest by the research community as have those of fixed wing aircraft, and most of the work in this field is based on classical work on helicopter aerodynamics [4], [5]. In [6] and [7], a model for induced drag is derived and a velocity estimator is implemented using this model, but they do not compensate for this induced drag in the control loop.

In [8], blade element momentum theory (BEMT) is used to derive a more precise thrust model for quadrotor propellers. However, this model is presented as a function of the induced velocity at the actuator disk, which is not characterized. Furthermore, no experimental data is used to validate this model.

We gratefully acknowledge the support of DARPA grants HR001151626/HR0011516850, ARL grant W911NF-08-2-0004, ARO grant W911NF-13-1-0350, ONR grant N00014-14-1-0510, and NSF grants 1426840/1521617.

J. Svacha, K. Mohta and V. Kumar are with the GRASP Lab, University of Pennsylvania, {jsvacha, kmohta, kumar}@seas.upenn.edu.

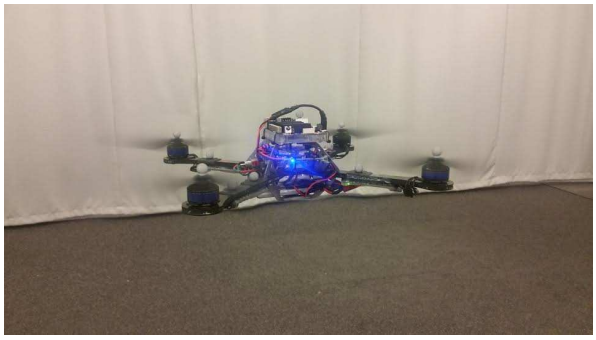

Fig. 1. The Ascending Technologies Hummingbird quadrotor used in our experiments.

In [9], the authors analyze and compensate for the aerodynamic effects on quadrotors, but they primarily look at performance during transient behavior such as is seen in stall turn maneuvers, whereas we look at reducing steady state errors during forward and vertical flight.

This work presents multiple contributions. We demonstrate that incorporating simple lumped parameter models for drag and propeller aerodynamics into the quadrotor dynamics and compensating for them in a control loop can reduce the RMS position error during tracking of constant-velocity trajectories by up to 75%. We show that this reduction in error is consistent over many repeated trials, validating models proposed in previous works that have not been extensively tested. We further demonstrate that the parameters for these models may be identified offline using flight data in which the mass and speed of the quadrotor are varied.

This paper is outlined as follows. In Section 2, we present the models used to characterize the varying aerodynamic effects on the quadrotor. In Section 3, we discuss system identification for these models and describe the experiments that we used to identify the model parameters. In Section 4, we discuss how these aerodynamics effects are compensated for in the control system. Finally, Section 5 describes the experimental results where we compare controllers with and without compensating for the modeled aerodynamic effects.

II. Aerodynamic Modeling

This section covers two topics: modeling the induced drag of a quadrotor and modeling the thrust variation due to the velocity of the quadrotor. We express vector quantities in one

of two coordinate systems: a right-handed world coordinate system $\mathcal{W}$ in which the x direction points North, the y direction points West, and the z direction points up, and a right-handed body coordinate system $\mathcal{B}$ where the origin is at the center of mass and the x direction is the front of the quadrotor, the y direction is to the left of the quadrotor and the z direction upwards as given by the right-hand rule. These coordinate frames can be seen in Figure 2.

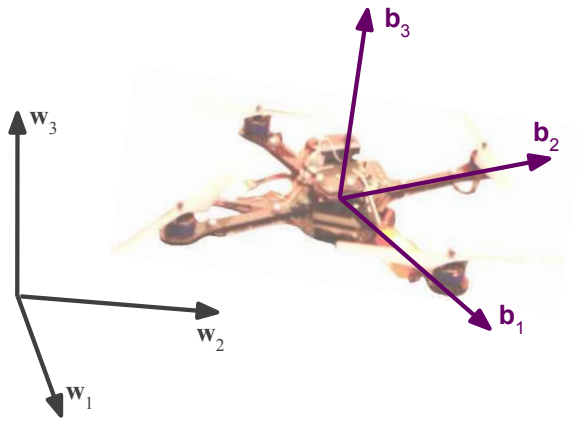

Fig. 2. World and body coordinate frames used to express vector quantities.

A. Linear Drag Model

We choose to compensate for the induced drag which, as shown in Figure 3, is in the x-y plane of the quadrotor.

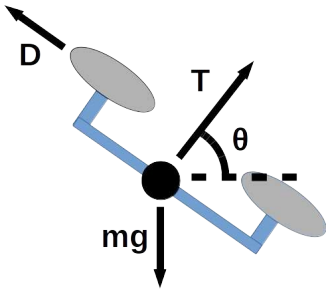

Fig. 3. Free body diagram of the quadrotor model showing the thrust, drag and gravitational forces.

The induced drag is linear in the body x-y velocity of the quadrotor. We make this decision because induced drag is simple to model and it has a significant effect on small-scale aerial vehicles with rigid blades [10]. In addition, many other sources of drag and drag-like effects may be approximated as linear in the body x-y velocity including blade flapping, profile drag, and translational drag, so this model captures them as well. We consider parasitic drag negligible in our flight regime. The model used for induced drag was proposed in [6] and further simplified in [7]. Using this model, the drag force $\mathbf{D}$ on the quadrotor is modeled as:

$$\mathbf{D} = -k_d \omega_s R P R^T \mathbf{V} \tag{1}$$

where $\mathbf{V}$ is the velocity of the quadrotor expressed in the world frame, k_d is the drag constant, R is the orientation of the quadrotor expressed as a rotation matrix which takes points from the body frame to the world frame, $\omega_s = \sum_{i=1}^{4} \omega_i$ is the sum of the motor speeds ω_i, and P is the projection matrix:

$$P = \begin{bmatrix} 1 & 0 & 0 \\ 0 & 1 & 0 \\ 0 & 0 & 0 \end{bmatrix}$$

The equations of motion for the quadrotor are then modified to include the drag force and moment:

$$\dot{\mathbf{V}} = \frac{F}{m} R \mathbf{e}_3 - g \mathbf{e}_3 - \frac{k_d}{m} \omega_s R P R^T \mathbf{V} \tag{2}$$

$$\dot{\mathbf{\Omega}} = J^{-1} \left(\mathbf{\Omega} \times J \mathbf{\Omega} - \mathbf{M} + \left(k_d \omega_s R P R^T \mathbf{V} \right) \times h \mathbf{e}_3 \right) \tag{3}$$

where m is the mass of the quadrotor, F is the magnitude of the applied thrust, $\mathbf{e}_3 = \begin{bmatrix} 0 & 0 & 1 \end{bmatrix}^T$ is the third standard basis vector, $\mathbf{\Omega}$ is the angular velocity vector expressed in the body frame, J is the inertia tensor in the body frame, $\mathbf{M}$ is the net applied moment, and h is the height of the propellers above the center of mass.

B. Thrust Model

We refer to the commonly used thrust model given by $T_i = k_\omega \omega_i^2$ as the "standard" thrust model, where T_i is the thrust produced by the i^{th} propeller and k_ω is a positive constant that is determined experimentally. A more accurate lumped parameter model derived using blade-element momentum theory in [8] is given by

$$T_i = c_1 \omega_i^2 \left(c_2 \left(1 + \frac{3}{2} \mu_i^2 \right) - \lambda_i \right) \tag{4}$$

where c_1 and c_2 are positive constants and μ_i and λ_i are the advance and inflow ratios, respectively. These are given:

$$\mu_i = \frac{V_{hi} + v_{hi}}{r \omega_i} \tag{5}$$

$$\lambda_i = \frac{V_{zi} + v_{zi}}{r \omega_i} \tag{6}$$

In the above equations, r is the radius of the propeller, V_{hi} and V_{zi} are the horizontal and vertical components of the velocity of the i^{th} propeller in the body frame, and v_{hi} and v_{zi} are the horizontal and vertical components, respectively, of the induced velocity through the ith propeller.

We make the following assumptions:

1) The propeller is sufficiently rigid so that the flapping angle is small, and the horizontal induced velocity $v_{hi} \approx 0$. Hence, the induced velocity of the i^{th} propeller becomes $v_i \approx v_{zi}$.
2) The induced velocity v_i is independent of the horizontal velocity V_{hi}, and is a function of the vertical speed of the propeller V_{zi} and motor speed ω_i. This is because V_{hi} is much smaller compared to the rotor tip speed than V_{zi} is compared to the induced velocity v_i, so V_{zi} dominates the effective angle of attack of the blade.

In order to find the relationship between v_i, ω_i and V_{zi}, we collected data by flying the quadrotor upwards and

downwards at varying speeds V_z from $-2\,\mathrm{m\,s^{-1}}$ to $2\,\mathrm{m\,s^{-1}}$ while logging the motor speeds ω_i. We also added small weights to the robot to get data with different values of the mass m. Then, we computed the induced velocity from momentum theory [5]:

$$T_i = 2\rho A v_i \left(v_i + V_z\right) \tag{7}$$

where ρ is the density of air, A is the area swept out by the propeller and for the constant velocity vertical flight, the thrust per propeller $T_i \approx mg/4$.

We plotted v_i against $\frac{1}{4}\omega_s$ and V_z, and found that a linear model fit the data well, with an adjusted R^2 value of 0.974. The regression is shown in Figure 4. Thus, we model v_i as linear in ω_i and V_{zi} with positive constants a and b:

$$v_i\left(\omega_i, V_{zi}\right) = a\omega_i - bV_{zi} \tag{8}$$

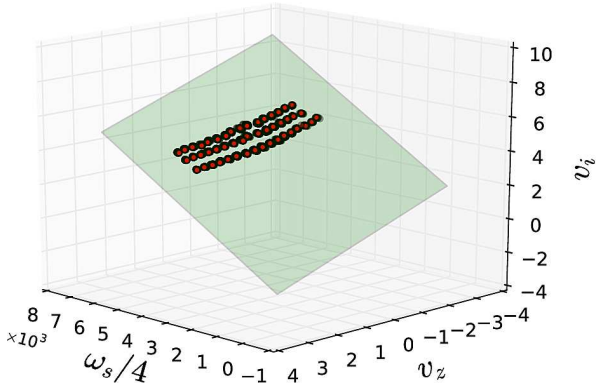

Fig. 4. Linear regression of the average induced velocity v_i against the average motor speed and the vertical velocity V_z.

Using (5), (6), (8) and the above mentioned assumptions, we can simplify (4) to the "refined" thrust model:

$$T_i = k_\omega \omega_i^2 - k_z V_{zi}\omega_i + k_h V_{hi}^2 \tag{9}$$

where k_ω, k_z, and k_h are positive constants that are determined experimentally.

III. System Identification

In this section we describe the design of the experiments used to identify the parameters of the models described in (1) and (9), i.e. the drag coefficient k_d and the thrust coefficients k_ω, k_z, and k_h.

A. Identifying the Induced Drag Coefficient

The drag coefficient k_d can be identified using accelerometer and velocity data during forward flight. The accelerometer measures the specific acceleration of the quad (the acceleration minus acceleration due to gravity), which is the acceleration due to thrust and the drag forces [7], plus a constant bias:

$$\mathbf{a}_{\mathrm{IMU}} = R^T(\dot{\mathbf{V}} + g\mathbf{e}_3) + \mathbf{b}_a \tag{10}$$

where $\mathbf{b}_a$ is the bias of the accelerometer. We may expand this expression by substituting (2) into it. In forward flight, the x component of $\mathbf{a}_{\mathrm{IMU}}$ becomes:

$$a_{\mathrm{IMU}x} = -\frac{k_d}{m}\omega_s V_x \cos\theta + b_{ax} \tag{11}$$

where V_x is the x component of the quadrotor velocity and θ is the pitch angle.

To identify k_d, we flew the quadrotor in hover and forward flight at speeds varying from $0\,\mathrm{m\,s^{-1}}$ to $8\,\mathrm{m\,s^{-1}}$ with increments of $0.25\,\mathrm{m\,s^{-1}}$ and fit a least squares linear model to the measured accelerometer, velocity, and commanded motor speed data. Only the data from the constant velocity segments of the trajectories was used in the linear regression. We assumed that the response of the motor controllers is fast so that the motor RPMs settle down to steady state values in the constant velocity segment of the trajectory. The data fit well with an R^2 value of 0.975, giving an estimate of the drag coefficient $\hat{k}_d = 1.314 \times 10^{-5}\ \frac{\mathrm{N{\cdot}s}}{\mathrm{m{\cdot}RPM}}$. The plot of this data is shown in Figure 5.

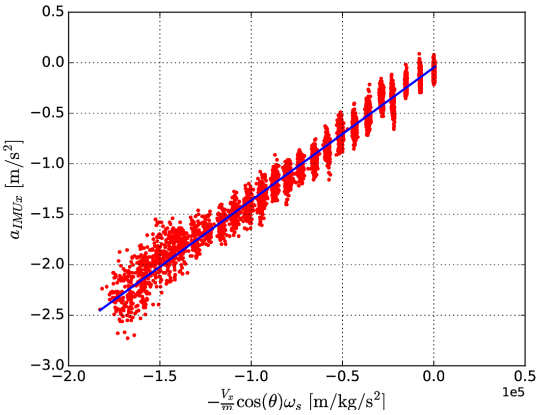

Fig. 5. Least squares linear regression used to compute the induced drag coefficient k_d.

B. Identifying the Thrust Coefficients

Summing (9) over all four propellers and assuming $V_{zi} = V_z$ and $V_{hi} = V_h$ (this is a good assumption when $\mathbf{\Omega} \approx 0$, which is satisfied in our experiments) gives:

$$\sum_{i=1}^{4} T_i = k_\omega \sum_{i=1}^{4} \omega_i^2 - k_z V_z \sum_{i=1}^{4} \omega_i + 4k_h V_h^2 \tag{12}$$

During the constant velocity vertical flight, $\sum_{i=1}^{4} T_i \approx mg$ and during horizontal flight, $\sum_{i=1}^{4} T_i \approx m \cdot a_{\mathrm{IMU}z}$, where $a_{\mathrm{IMU}z}$ is the z reading of the accelerometer, assuming that the accelerometer bias is small. The thrust coefficients k_ω, k_z, and k_h were identified by fitting a least squares linear model to vertical and forward flight data using (12), in which all the other quantities are known. The quality of the fit was very good with an R^2 value of 0.955. A plot of a linear regression used to compute the parameters k_ω and k_z from vertical flight data is shown in Figure 6. The identified parameter values are $\hat{k}_\omega$ =

$8.00 \times 10^{-8}\,\mathrm{N/RPM^2}$, $\hat{k}_z = 2.55 \times 10^{-5}\,\mathrm{N\,s/m/RPM^2}$, and $\hat{k}_h = 3.39 \times 10^{-3}\,\mathrm{N\,s^2/m^2}$.

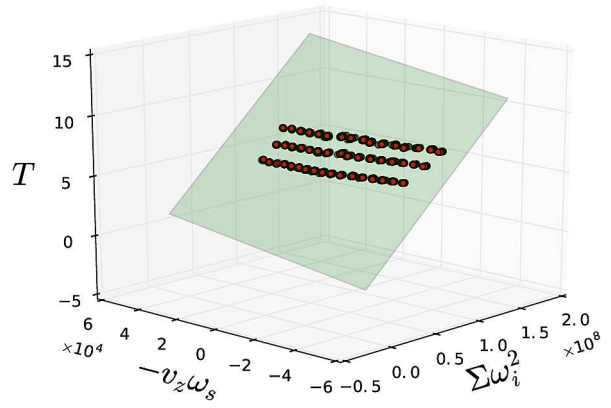

Fig. 6. Linear regression used to compute a and b from vertical flight data.

IV. Aerodynamic Compensation

Once we have models of the aerodynamic effects acting on the quadrotor, we modify the controller to compensate for the effects predicted by the drag and thrust models discussed in Section II. The controller used is a modification of the controller presented in [11] and [12].

A. Drag Compensation

The acceleration commanded by the controller is given:

$$\mathbf{a}_{\text{cmd}} = \mathbf{a}_{\text{des}} - K_v\mathbf{e}_v - K_x\mathbf{e}_x \tag{13}$$

where $\mathbf{a}_{\text{des}}$ is the desired acceleration of the trajectory, K_v and K_x are positive semidefinite gain matrices, and $\mathbf{e}_v = \mathbf{V} - \mathbf{V}_{\text{des}}$ and $\mathbf{e}_x = \mathbf{x} - \mathbf{x}_{\text{des}}$ are the velocity and position errors, respectively. Substituting in the acceleration from (2), we want the commanded force, F_{cmd}, to satisfy:

$$F_{\text{cmd}}R\mathbf{e}_3 = \underbrace{m(\mathbf{a}_{\text{des}} - K_v\mathbf{e}_v - K_x\mathbf{e}_x + g\mathbf{e}_3)}_{\boldsymbol{\alpha}} - k_d\omega_s RPR^T\mathbf{V} \tag{14}$$

We wish to determine the thrust F_{cmd} that we should command in order to follow the desired trajectory. In general, the above equation cannot be exactly satisfied by selecting F_{cmd} because the vectors on the left and the right hand side are not aligned. The best we can do is project each side onto $R\mathbf{e}_3$. Doing this and noticing that $(RPR^T\mathbf{V})^T R\mathbf{e}_3 = 0$, we get:

$$F_{\text{cmd}} = \boldsymbol{\alpha}^T R\mathbf{e}_3 \tag{15}$$

where $\boldsymbol{\alpha}$ is as shown in (14).

This is the same equation that is used to compute the desired thrust in the controller without drag. This happens because the drag force is orthogonal to the thrust vector, so the thrust vector cannot directly compensate for the drag. To compute the desired attitude, we wish to find the commanded attitude R_{cmd} such that there exists an F_{cmd} such that:

$$F_{\text{cmd}}R_{\text{cmd}}\mathbf{e}_3 + k_d\omega_s R_{\text{cmd}}PR_{\text{cmd}}^T\mathbf{v} = \boldsymbol{\alpha} \tag{16}$$

In this case, $R_{\text{cmd}} = \begin{bmatrix}\mathbf{b}_{1c} & \mathbf{b}_{2c} & \mathbf{b}_{3c}\end{bmatrix}$, where $\mathbf{b}_{ic}$ is the i^{th} basis vector of the body frame. If we left-multiply each side of the above equation by R_{cmd}^T, this becomes three equations:

$$F_{\text{cmd}} = \mathbf{b}_{3c}^T\boldsymbol{\alpha} \tag{17}$$

and

$$\mathbf{b}_{1c}^T(k_d\omega_s\mathbf{V} + \boldsymbol{\alpha}) = 0 \tag{18}$$

$$\mathbf{b}_{2c}^T(k_d\omega_s\mathbf{V} + \boldsymbol{\alpha}) = 0 \tag{19}$$

Equations (18) and (19) indicate that $\mathbf{b}_{1c}$ and $\mathbf{b}_{2c}$ are both orthogonal to the vector $k_d\omega_s\mathbf{V} + \boldsymbol{\alpha}$. This means that $\mathbf{b}_{3c}$ is aligned with this vector:

$$\mathbf{b}_{3c} = \pm\frac{\omega_s\mathbf{V} + \boldsymbol{\alpha}}{\|\omega_s\mathbf{V} + \boldsymbol{\alpha}\|} \tag{20}$$

To resolve the sign ambiguity, we choose the direction that makes F_{cmd} nonnegative in equation (17). $\mathbf{b}_{1c}$ and $\mathbf{b}_{2c}$ can then be chosen from the desired yaw.

If the rotor height h is significant, we can modify the controller [11] to add a feed-forward moment $\mathbf{M}_d$ to the commanded moment in order to compensate for the drag induced moment:

$$\mathbf{M}_d = h\mathbf{e}_3 \times \left(k_d\omega_s RPR^T\mathbf{V}\right) \tag{21}$$

B. Thrust Compensation

To compensate for thrust according to the model, we make the assumption that the counter-moment M_i of the ith propeller is proportional to the thrust of that propeller T_i by the constant k_M:

$$M_i = k_M T_i \tag{22}$$

For the configuration of the quadrotor in which motor the motors are numbered 1 through 4, increasing index in the counterclockwise direction and with motor 1 being the front motor, the equation that relates the net thrust F and net moments M_x, M_y, and M_z to the individual thrusts T_i is given by[13],

$$\begin{bmatrix} F \\ M_x \\ M_y \\ M_z \end{bmatrix} = \begin{bmatrix} 1 & 1 & 1 & 1 \\ 0 & L & 0 & -L \\ -L & 0 & L & 0 \\ k_M & -k_M & k_M & -k_M \end{bmatrix} \begin{bmatrix} T_1 \\ T_2 \\ T_3 \\ T_4 \end{bmatrix} \tag{23}$$

Given the net thrust and net moment, (23) may be inverted to compute T_1 through T_4. Then, using known V_z and V_h, we may solve

$$T_i = k_\omega\omega_i^2 - k_z V_z\omega_i + k_h V_h^2 \tag{24}$$

for ω_i in closed form since it is quadratic in ω_i.

V. Experimental Results

This section discusses experimental results for controllers designed to compensate for the aforementioned aerodynamic effects of drag and propeller thrust variation with velocity. For these tests, we flew an Ascending Technologies Hummingbird due to its light weight and agility. For on board computation and data logging we added an Odroid C2 unit

to the robot due to its light weight and high computing power. The propellers selected for the vehicle are the black AR Drone 2.0 propellers, which were chosen because of their availability. The computation of position control inputs was done externally on a base station, and the commanded attitude and desired thrust force were transmitted to the quadrotor using 2.4 GHz wireless communication. The desired thrust and orientation are used by the orientation controller running on the robot to compute the desired motor speeds.

A. Drag Compensation Tests

In order to evaluate the performance of the drag compensating controller, the quadrotor was flown on 25 forward flight trajectories with and without drag compensation. The velocity profile of the trajectories is shown in Figure 7. The x and z position errors are shown in Figures 8 and 9, respectively.

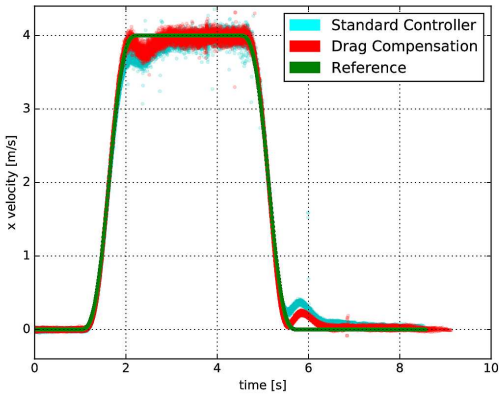

Fig. 7. x velocity for forward flight with and without drag compensation.

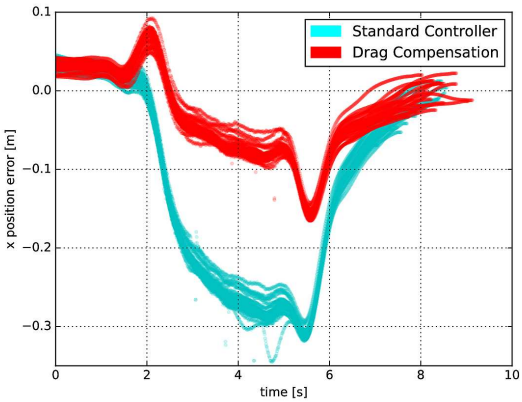

Fig. 8. x position error for forward flight with and without drag compensation.

Figure 8 indicates that, for the steady state velocity segment, the drag compensating controller reduces the magnitude of the x position error from an RMS value of $26\,\mathrm{cm}$ to $6.6\,\mathrm{cm}$. As Figure 9 shows, the z position error is slightly affected by drag compensation. It should be noted that the nominal z position error is between 0 and $5\,\mathrm{cm}$ due to the sensitivity of the controller to k_ω. In our case, k_ω is perhaps slightly below the actual value, causing the quadrotor to apply slightly more thrust when the z position error is zero.

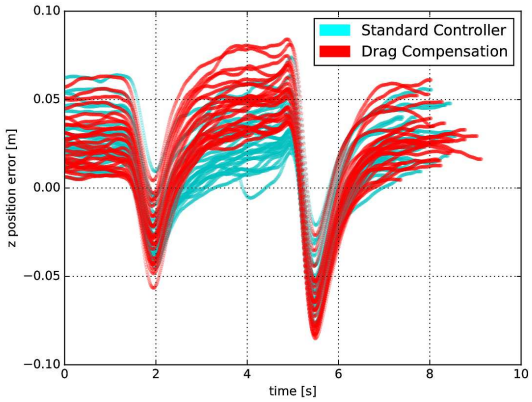

Fig. 9. z position error for forward flight with and without drag compensation.

B. Refined Thrust Model Tests

The quadrotor was also flown on 25 forward flight trajectories with and without the refined thrust model, in all cases using drag compensation. This was done to determine whether the refined thrust model further improved tracking performance. The trajectories were the same as described in the previous subsection. The velocity profile is shown in Figure 10. The x and z position errors are shown in Figures 11 and 12, respectively.

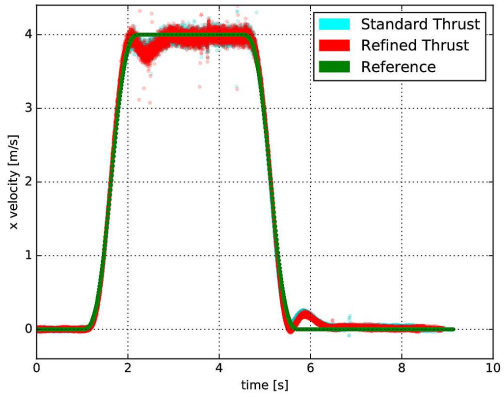

Fig. 10. x velocity for forward flight with standard and refined thrust models (both with drag compensation enabled).

Figure 11 shows no significant difference in x position tracking performance between the standard and the refined thrust models, which had RMS x position errors of $6.6\,\mathrm{cm}$ and $6.5\,\mathrm{cm}$, respectively. The refined thrust model slightly worsens the z tracking performance in this case, resulting in

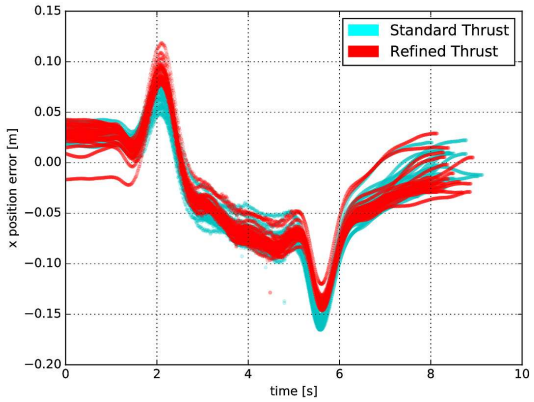

Fig. 11. x position error for forward flight at $4\,\mathrm{m\,s^{-1}}$ with standard and refined thrust models (both with drag compensation enabled).

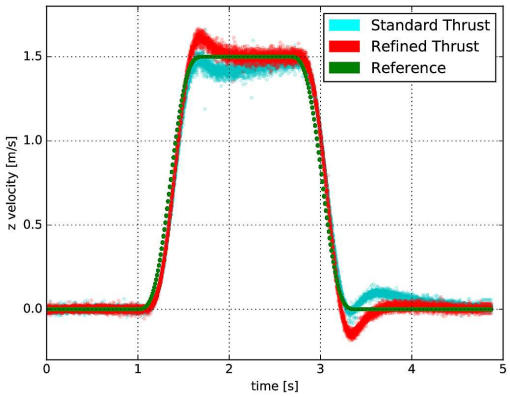

Fig. 13. z velocity for forward flight at $1.5\,\mathrm{m\,s^{-1}}$ with standard and refined thrust models (both with drag compensation)

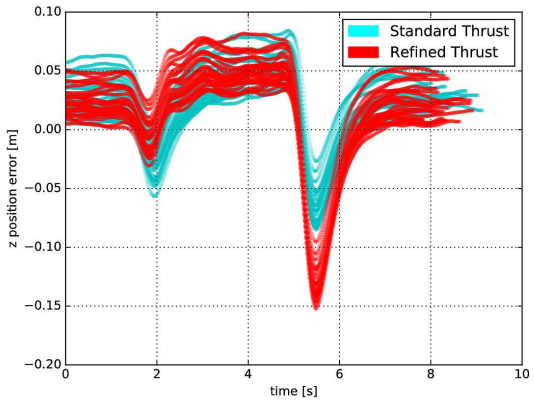

Fig. 12. z position error for forward flight at $4\,\mathrm{m\,s^{-1}}$ with standard and refined thrust models (both with drag compensation enabled).

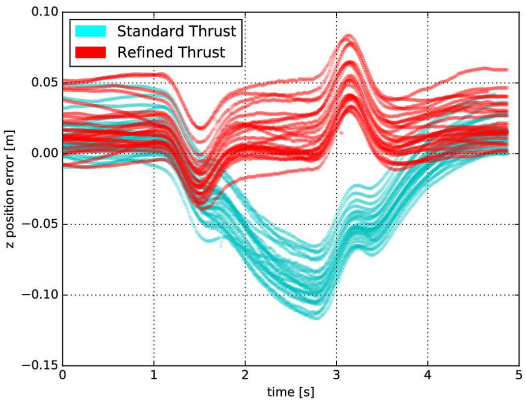

Fig. 14. z position error for forward flight at $1.5\,\mathrm{m\,s^{-1}}$ with standard and refined thrust models (both with drag compensation)

a larger drop in height during the deceleration phase of the trajectory.

The quadrotor was flown on 25 vertical flight trajectories with and without the refined thrust model, using only the k_ω and k_z terms (k_h is ineffective in vertical flight). Figure 13 shows the velocity profile for the trajectory we used, and Figure 14 shows the z position error for the trajectories.

Figure 14 shows that the z position error is significantly reduced from an RMS value of $7.3\,\mathrm{cm}$ with the standard thrust model to $2.0\,\mathrm{cm}$ with the refined thrust model. It is suspected that the bumps in position error during the acceleration and deceleration phases of the trajectory are caused by the ramp-up and ramp-down times for the motor speeds.

Table I shows an overview of the root-mean-square (RMS) errors in steady state flight for different trajectories using different forms of compensation.

VI. Conclusion

In this work, we have shown that we can significantly reduce the position error in the direction of forward flight by incorporating a simple drag model into the quadrotor dynamics and changing the commanded attitude to compensate for this drag. In addition, we have shown that the z position error can be reduced in vertical flight by incorporating a simple lumped parameter model that assumes that the induced velocity v_i is linear in the vertical speed in the body frame V_z and the motor speed ω_i. We have shown that all of these parameters are easy to identify by fitting a model to flight data using linear regression.

Future work involves determining the observability properties of k_d, k_ω, k_z, and k_h and estimating these parameters during flight using a nonlinear observer or an unscented Kalman filter. In addition, we wish to investigate and compensate for the effects of parasitic drag on the quadrotor at flights of even higher speeds of up to 20 m/s.

References

[1] J. Nikolic, M. Burri, J. Rehder, S. Leutenegger, C. Huerzeler, and R. Siegwart, "A uav system for inspection of industrial facilities," in *2013 IEEE Aerospace Conference*, March 2013, pp. 1–8.

[2] S. K. Sarkar, J. Das, R. Ehsani, and V. Kumar, "Towards autonomous phytopathology: Outcomes and challenges of citrus greening disease

TABLE I

THE RMS ERRORS IN THE x AND z POSITION WHEN FLYING FORWARD AND VERTICAL TRAJECTORIES USING THE CONTROLLERS PROPOSED IN OUR WORK.

Trajectory	**Controller**	x **error [cm]**	z **error [cm]**
forward	standard	26.0	3.0
forward	drag	6.6	4.7
forward	drag + thrust	6.5	5.1
vertical	standard	-	7.3
vertical	thrust	-	2.0

detection through close-range remote sensing," in *IEEE International Conference on Robotics and Automation*, May 2016.

[3] S. Gupte, P. I. T. Mohandas, and J. M. Conrad, "A survey of quadrotor unmanned aerial vehicles," in *2012 Proceedings of IEEE Southeastcon*, March 2012, pp. 1–6.

[4] W. Johnson, *Helicopter Theory*. Princeton University Press, 1980.

[5] G. J. Leishman, *Principles of Helicopter Aerodynamics*, 2nd ed. Cambridge University Press, 2006.

[6] P. Martin and E. Salaun, "The true role of accelerometer feedback in quadrotor control," in *Proc. IEEE International Conference on Robotics and Automation (ICRA)*, Anchorage, Alaska, May 2010, pp. 1623–1629.

[7] R. Leishman, J. C. Macdonald, Jr., R. Beard, and T. McLain, "Quadrotors and accelerometers: State estimation with an improved dynamic model," *IEEE Control Systems Magazine*, vol. 34, Feb. 2014.

[8] M. Bangura, M. Melega, R. Naldi, and R. Mahony, "Aerodynamics of rotor blades for quadrotors," 2016, arXiv:1601.00733.

[9] H. Huang, G. M. Hoffmann, S. L. Waslander, and C. J. Tomlin, "Aerodynamics and control of autonomous quadrotor helicopters in aggressive maneuvering," in *IEEE Conference on Robotics and Automation*, Kobe, Japan, May 2009.

[10] M. Bangura and R. Mahony, "Nonlinear dynamic modeling for high performance control of a quadrotor," in *Proc. Australasian Conference on Robotics and Automation*, Victoria University of Wellington, New Zealand, Dec. 2012.

[11] T. Lee, M. Leok, and N. H. McClamroch, "Geometric tracking control of a quadrotor uav on se(3)," in *Proc. 49th IEEE Conference on Decision and Control*, Atlanta, Georgia, Dec. 2010.

[12] D. Mellinger and V. Kumar, "Minimum snap trajectory generation and control for quadrotors," in *2011 IEEE International Conference on Robotics and Automation*, May 2011, pp. 2520–2525.

[13] N. Michael, D. Mellinger, Q. Lindsey, and V. Kumar, "The GRASP Multiple Micro-UAV Testbed," *IEEE Robotics Automation Magazine*, vol. 17, no. 3, pp. 56–65, Sept 2010.